J Fail. Anal. and Preven. (2019) 19:882–889
https://doi.org/10.1007/s11668-019-00689-9

CASE HISTORY—PEER-REVIEWED

Failure Analysis of Metallic Components of a Battery Fitted in a Naval System

Mrityunjoy Hazra · Satyapal Singh

Submitted: 16 January 2019 / Accepted: 8 August 2019 / Published online: 30 August 2019

Abstract A battery based on Mg–AgCl with sea water as electrolyte was developed for propulsion of a naval system. In one occasion, the tie rod, conduit pipe and the copper bus rod each covered with polymer sleeve were found damaged. The copper bus rod was melted probably by amplified resistance and subsequent heating. Localized cross-sectional reduction (and thus increased resistance, R) seems to have aggravated heating by Joule heating ($J = I^2R$) effect. Subsequently, it led to partial dissolution, embrittlement, softening and final fracture of the steel tie rod in the said sequence. There was no material deficiency. Chemical composition, microstructure and hardness values of the failed components indicate that the steel tie rod was made of the as-specified EN 24 type of low alloy steel in hardened and tempered condition, while copper bus rods were made of pure copper of 99.50% purity. Damage of the conduit tube was not related to the failure of steel tie rod and copper bus rod, although it indirectly offers clues that melting of copper happened and the molten copper reached many locations within the system.

Keywords Failure · Metallic component · Battery · Liquid metal embrittlement (LME) · En 24 steel · Copper bus rod

M. Hazra (✉) · S. Singh
Defence Metallurgical Research Laboratory (DMRL), P.O. – Kanchanbagh, Hyderabad 500 058, India
e-mail: mhazra@dmrl.drdo.in; hazra.mrityunjoy@gmail.com

Introduction

A battery based on Mg–AgCl with sea water as electrolyte was developed for propulsion of a naval system. The construction of this battery involves steel tie rods, titanium conduit pipes and copper bus rods (Fig. 1), and each of these components was covered with a polymer sleeve. In one occasion during start of a trial, the tie rod, conduit pipe and the copper bus rod were found damaged. The damaged parts were received at this laboratory for investigation on cause of the damage.

Experimental Procedure

The failed steel tie rod, copper bus rods and titanium conduit pipe were, at first, examined visually by naked eye and under magnifying glass. Photographs in the as-received condition were taken and preserved for future reference, during the course of analysis. The failed parts were then sectioned from the main components for its further analysis. Later, those parts were put under forced air using air-blower to remove the loosely adhered particles and then examined under scanning electron microscope (SEM). Fracture surface was cleaned ultrasonically in acetone after examination on probable surface corrosion debris and/or contamination, before fractographic study. Branson solution was used for removal of thick corrosion product so as to reveal the fractograph in a better way. After that, representative cross-sectional sample extraction from failed parts was carried out from near to the failed surface as well as from away from the failure location for detailed metallographic (optical microscopic and scanning electron microscopic) study in both unetched and etched conditions.

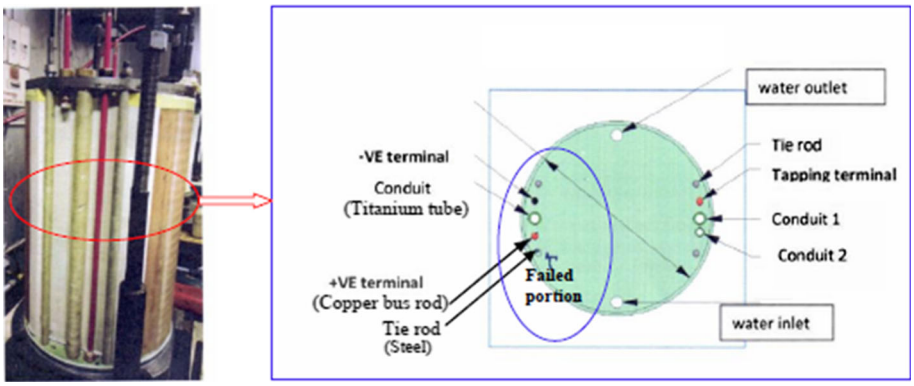

Fig. 1 Positions of the failed steel tie rod, copper conductor rod and titanium conduit tube, as seen in a transverse sectional view of the battery

Bulk compositional analysis of the tie rod and bus rods was carried out by inductively coupled plasma–optical emission spectroscopy (ICP–OES) type wet chemical analysis technique. Compositional analyses on each phase in microstructure were carried out with electron-dispersive spectroscopy (EDS) attachment of the SEM. Steel tie rod was etched with 3% nital, while acidified potassium dichromate was used for etching copper conductor rod. Vickers microhardness readings at 1 kgf were taken on metallographically prepared samples to correlate those with the respective microstructures so as to obtain a reasonably complete idea about the material.

Results

Visual Examination

Figures 2–5 show photographs of the failed components in as-received condition. Figure 2 shows three failed parts, titanium conduit tube, steel tie rod and copper bus rod. Through hole is observed on titanium tube. No other metallic deposition was observed on the areas surrounding the hole. Mating failed surfaces of the tie rod and bus rod has been marked as 1 and 2.

Figure 3a and b shows tie rod failed surfaces 1 and 2, respectively. A reduction in cross section is clearly visible on failed surface 1 (Fig. 3a). On the other hand, a brownish deposit is found on mating surface 2 (Fig. 3b). Figure 4a and b shows copper bus rod failed surfaces 1 and 2, respectively. A loss of area is observed on failed surface 2 (Fig. 4b), while mating surface 1 exhibits a sharp tipped cone type of appearance (Fig. 4a). It is also noteworthy that the base of the said conical-shaped feature is at locations away from the bus rod original surface and a plane surface joins the two. In other words, the surface joining the cone and bus rod surface is a plane one and has an appearance of a properly machined surface. Figure 5 shows locally damaged portion of the titanium conduit tube. The damaged surface revealed very rough appearance. Very clear evidence of the presence of peeled off polymer sleeve is seen. Also, traces of reddish-brownish deposit were also seen, as marked in Fig. 5.

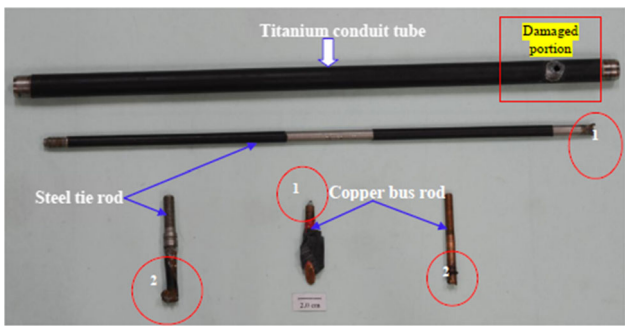

Fig. 2 Photographs of the as-received failed components

Fractography

Figures 6 and 7 show failed copper surfaces as observed under SEM. Signature of melting and re-solidification is vivid in each of the surfaces. Figures 8–11 present SEM images of the failed SS tie rod surface 1, shown in Fig. 2. Evidence of melted and resolidified copper along with rust was prevalent in major part of the periphery of the SS tie rod cross section (Fig. 8). This has been consistently supported by the EDS spectra taken from various regions on the failed surface. The magnified view of the box marked region in Fig. 8 is shown in Fig. 9. Intergranular failure is observed in that region. Some of the big granular steel fracture facets were found to be covered with a layer of melted and resolidified fine copper grains (Fig. 10). Other portion of the fracture surface exhibited ductile overload fracture (Fig. 11). Damaged part of the tube as seen under SEM, after cleaning with Branson liquid, is shown in Fig. 12. Evidence of corrosion is well revealed by both appearance of the damaged surface and EDS analysis. Trace amount of copper is revealed in EDS analysis as well.

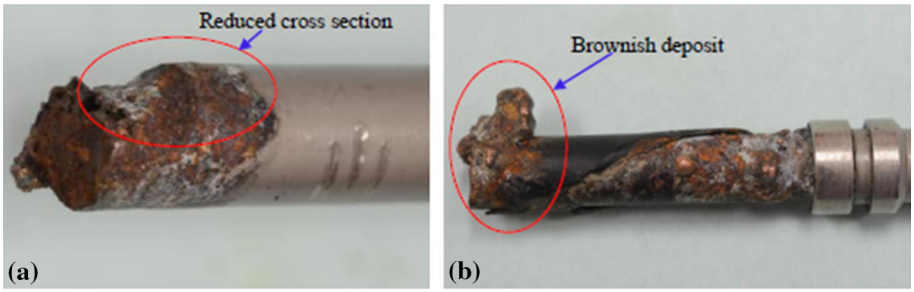

Fig. 3 Magnified views of as-received failed steel tie rod surfaces 1 and 2

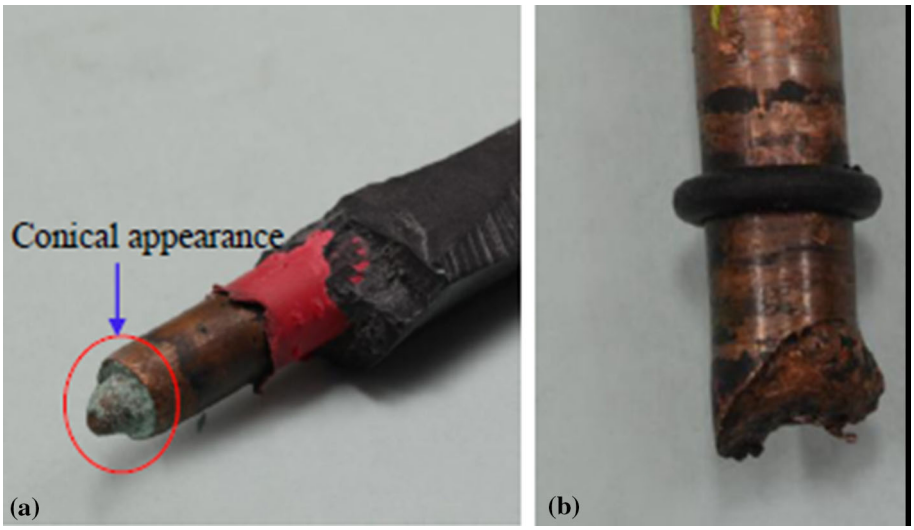

Fig. 4 Magnified views of as-received failed copper conductor rod surfaces 1 and 2

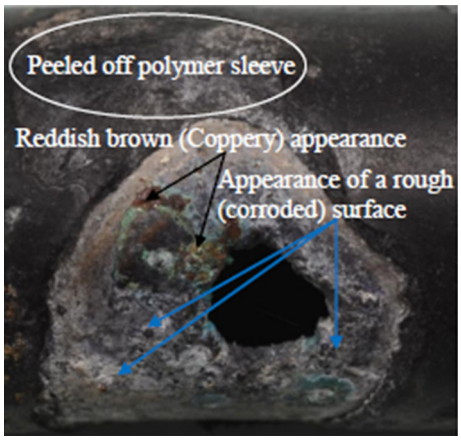

Fig. 5 Magnified view of as-received (locally damaged) titanium conduit tube

Microstructure

Figure 13a and b shows longitudinal metallographic section of the steel tie rod in unetched condition for two different locations. One may notice here that stringer types of inclusions are present in the whole structure. EDS analysis under SEM reveals those to be the alumina type (Fig. 14). Inclusion type was found to be of 2B thin type, as per ASTM E 45.

Microstructure of the locations far away from the failure reveals the presence of tempered martensite, after etching with 3% nital (Fig. 15a). On the other hand, microstructure at close to the failure region showed difference in contrast when compared to that at far away from the failure (Fig. 15b). A sharp boundary is noticed between these two varieties of microstructure (Fig. 15b), when etched and examined repeatedly for several times. Copper bus rod microstructure after etching with acidified potassium dichromate reveals the presence of alpha copper grains with twins (Fig. 16a), at location far away from the failure location. Figure 16b shows microstructure of a longitudinal section at close to the failed surface. Here, one can notice the melted and resolidified fine copper grains, in sharp contrast to the microstructure at away from the failed surface.

Chemical Composition

Tables 1 and 2 show chemical compositions of the steel tie rod and copper bus rod, respectively, obtained by wet analysis employing inductively coupled plasma–optical emission spectroscopy (ICP–OES) technique. Table 3 provides quantity of oxygen and nitrogen present in the copper bus rod, obtained by dry analysis method using LECO gas analyzer.

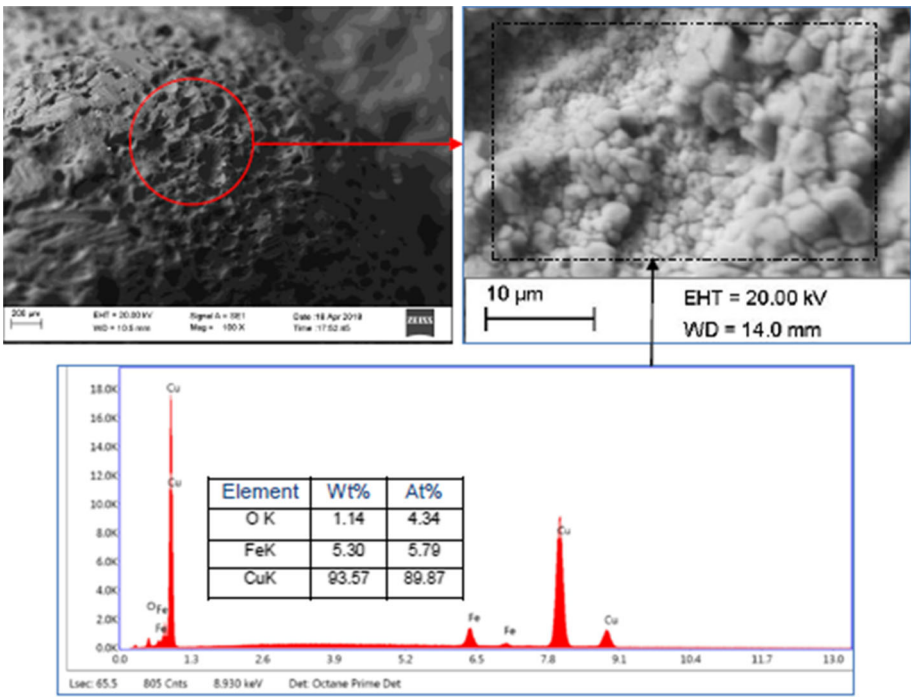

Fig. 6 Failed surface 2 of copper conductor rod as seen under SEM

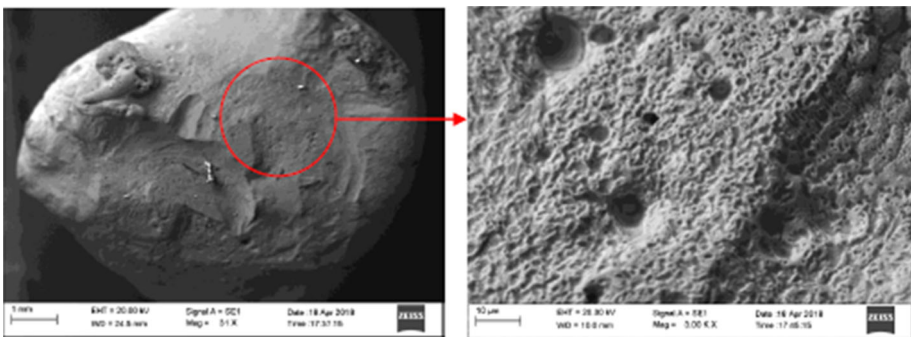

Fig. 7 Failed surface 1 of copper conductor rod as seen under SEM

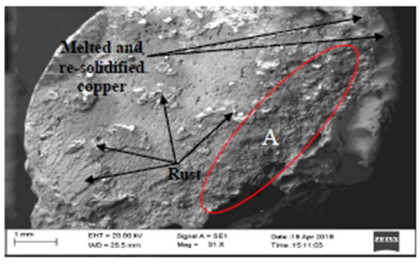

Composition of melted and resolidified copper

Element	Wt %	At%
O K	7.18	22.11
AlK	0.35	0.63
SiK	4.98	8.73
ClK	0.18	0.25
FeK	5.35	4.72
CuK	81.97	63.56

Composition of rust

Element	Wt %	At %
O K	18.23	43.62
ClK	0.72	0.78
CrK	0.93	0.69
FeK	80.11	54.91

Fig. 8 Failed surface 1 of steel tie rod as seen under SEM

Hardness

Vickers hardness values taken at 1 kgf load are 300 HV and 70 HV for steel tie rod and copper bus rod, respectively, at locations far away from the failed surfaces (Figs. 15, 16). The hardness values at close to the failed ends of the tie rod and copper bus rod are 500 HV and 50 HV, respectively.

Discussion

Material Identification

Chemical composition, microstructure and hardness values of the failed components indicate that the steel tie rod was made of the as-specified EN 24 type of low alloy steel in hardened and tempered condition, while copper bus rods were made of pure copper of 99.50% purity.

Failure Mechanism

Sequence of the events in the failure phenomenon looks to be as follows: (1) copper rod adjacent to the steel tie rod

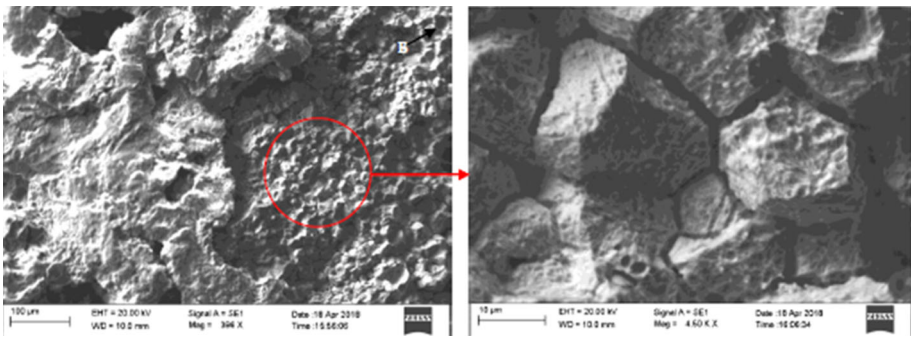

Fig. 9 Magnified view of the circled region A in Fig. 8

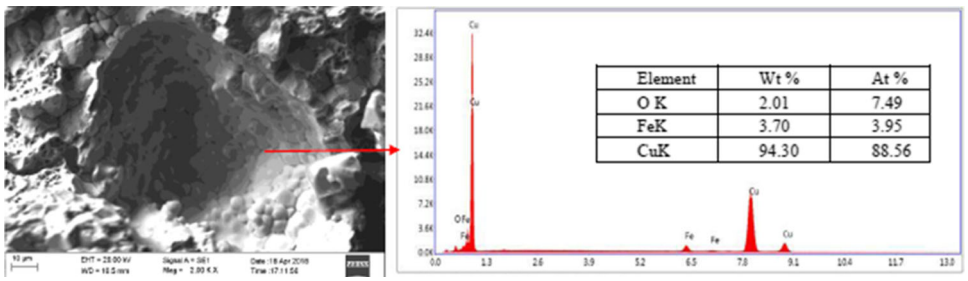

Element	Wt %	At %
O K	2.01	7.49
FeK	3.70	3.95
CuK	94.30	88.56

Fig. 10 Magnified view of the boxed region B in Fig. 9

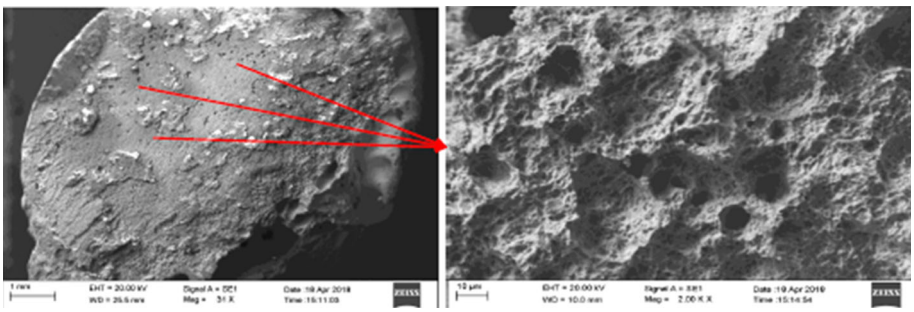

Fig. 11 Final overload fracture surface

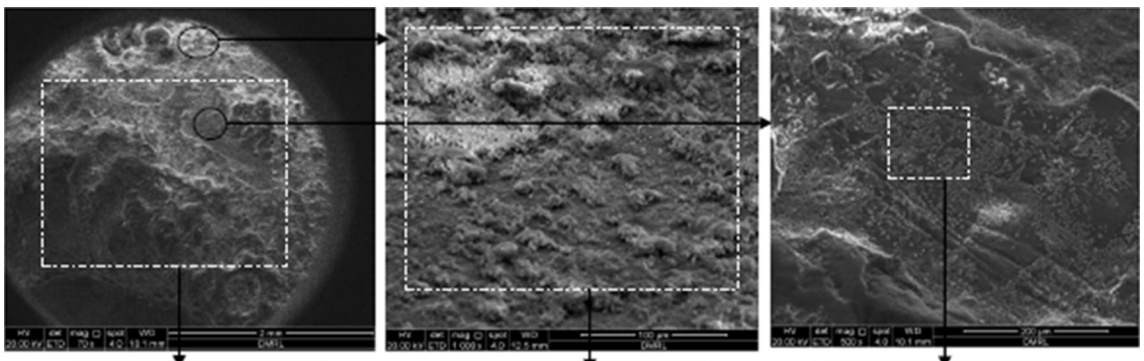

Element	Wt %	At %
O K	44.15	56.61
NaK	16.85	15.04
MgK	23.47	19.80
SiK	1.29	0.94
P K	1.72	1.14
ClK	7.03	4.07
CaK	1.83	0.94
TiK	2.69	1.15
CuK	0.90	0.32
Total	100.00	100.00

Element	Wt %	At %
O K	42.77	58.70
NaK	11.85	11.31
MgK	12.56	11.34
SiK	4.12	3.22
P K	2.94	2.08
ClK	5.39	3.34
CaK	7.42	4.06
TiK	12.96	5.94
Total	100.00	100.00

Element	Wt %	At %
O K	37.62	49.61
NaK	22.59	20.67
MgK	21.96	19.05
SiK	1.11	0.83
P K	0.35	0.24
ClK	14.59	8.68
CaK	1.16	0.61
TiK	0.68	0.30
Total	100.00	100.00

Fig. 12 Damaged (local) surface of titanium conduit tube as seen under SEM

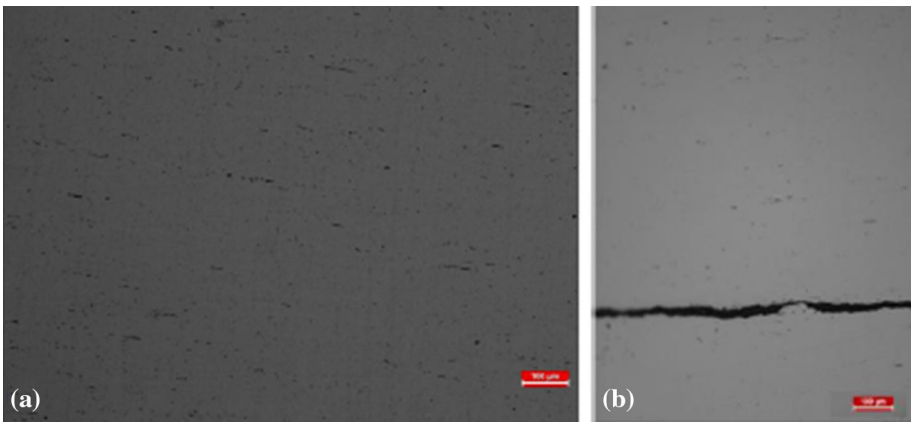

Fig. 13 Longitudinal steel tie rod section at two different locations (**a**, **b**), as observed under optical microscope. Unetched

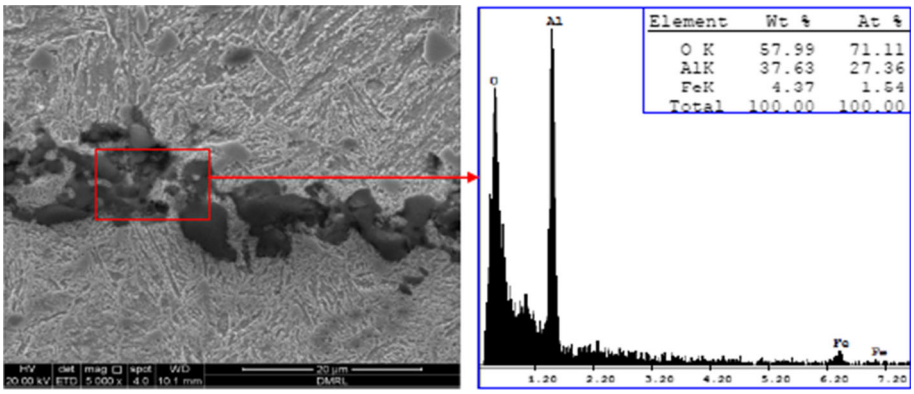

Fig. 14 Magnified view of the inclusion seen in Fig. 13b, as observed under SEM

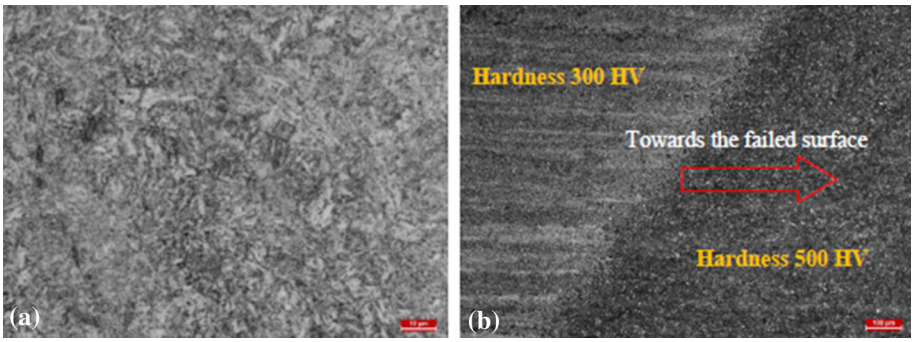

Fig. 15 Longitudinal steel tie rod section along with the failed surface, as observed under optical microscope. Etchant: 3% nital

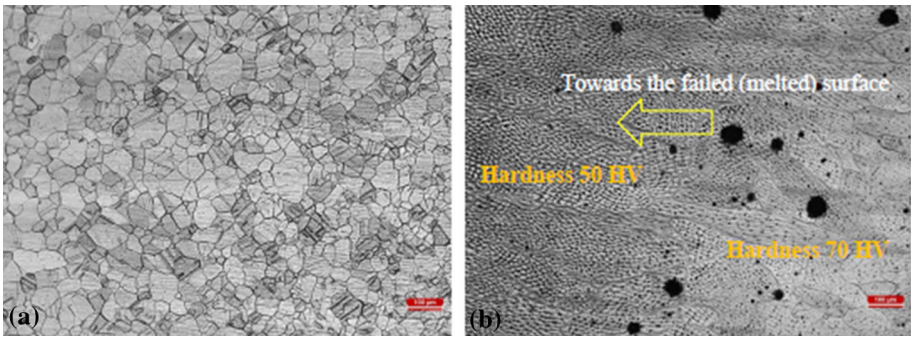

Fig. 16 Longitudinal copper conductor rod section along with the failed surface, as observed under optical microscope. Etchant: acidified potassium dichromate

Table 1 Chemical composition of steel tie rod

Sample ID	Chemical composition (wt.%)								
	C	S	P	Si	Mn	Cr	Mo	Ni	Fe
Steel tie rod	0.36	0.040	0.023	0.96	0.47	1.02	0.18	1.15	Bal.

Table 2 Chemical composition of copper bus rod

Sample ID	Chemical composition (wt.%)					
	Si	Ni	Pb	Co	Sn	Cu
Copper bus rod	0.18	0.013	0.06	0.0003	0.17	Bal.

Table 3 Trace element content of copper bus rod

Sample ID	Content (ppm)	
	O	N
Copper bus rod	150	25

melted probably due to localized higher resistance heating (Figs. 8, 10), (2) molten copper came in contact with the steel tie rod and dissolved part of the tie rod and thus resulted in reduction in tie rod cross section (Fig. 3a), (3) liquid copper also caused embrittlement in the tie rod in the next step leading to the intergranular fracture (Figs. 8, 9), (4) remaining section of tie rod failed due to overload caused (Fig. 11). The final (overload) fracture has been assisted by three prior events, viz. (a) reduced cross section due to partial consumption of the rod by molten copper, (b) intergranularly failed part of the cross section, and (c) elevated temperature of the tie rod coming in contact with the molten copper and resultant material softening. Intergranular fracture is an indication of extreme material embrittlement that happens along the material grain boundary. In the present case, it seems that liquid metal embrittlement (LME) by melted copper has led to the intergranularity of the steel fracture [1, 2]. The exposure of the steel tie rod to elevated temperature is evident from the fact that the fractured ends of the rod got hardened (500 HV hardness, Fig. 15) as compared to the locations away from the fractured end (300 HV hardness). This has probably happened as a result of austenitizing at some temperature by effect of molten copper, subsequent water quenching by available sea water and low temperature or nil tempering. This is quite plausible when one considers the as-specified heat treatment schedule of the steel tie rod (austenitizing at 860 °C/3 h + oil quenching, tempering at 580 °C/3 h + air cool) and hardness level (300 HV), as was provided by the user. However, this hardening is most likely to be a post-fracture event. And thus, in the process of austenitizing upon influence of molten copper, at first, the steel rod got softened by the elevated temperature. This softening also contributed to the tie rod fracture.

Damage of the titanium conduit tube is a separate phenomenon and has no relationship with fracture of the steel tie rod, as is clear from observations on failure type, failure nature and arrangement of components within the battery chamber (Fig. 1). However, it indirectly indicates the melting of copper rod and deposition of the same on the titanium tube, as is supported by Figs. 5 and 12. Damage of the tube seems to have happened by the following sequence: (1) steel tie rod melted and got deposited on the tube, (2) polymer sleeve in contact with the molten copper got damaged and the tube became exposed to the hot molten metal, (3) creation of a very rough surface under the action of molten copper on titanium surface, (4) subsequent failure (thinning of the tube and creation of a hole) happened by corrosion of the tube under Mg–AgCl and/or sea water.

On Shape of Copper Rod and Its Melting

There is a conical-shaped feature of one failed copper rod surface (Fig. 4a), in middle of the copper rod and a uniform annular surface at periphery. One plausible cause of formation of such feature could be a uniform cut in the copper rod. The reduced cross section of the copper rod would have increased the localized electrical resistance significantly.

Thus, localized cross-sectional reduction (and thus increased resistance, R) would lead to the aggravated heating by Joule heating ($J = I^2R$) effect.

Conclusion

The copper bus rod might have melted by amplified resistance and subsequent heating. Subsequently, it led to partial dissolution, embrittlement, softening and final fracture of the steel tie rod in the said sequence.

Recommendation

It is desirable to inspect the copper terminal rod for any surface damage before placing sleeve on the rod.

Acknowledgment The authors would like to thank Dr. Vikas Kumar, Distinguished Scientist (DS) and the Director, DMRL for his constant encouragement to work on the present field. Also, funding from DRDO is gratefully acknowledged.

References

1. B. Joseph, M. Picat, F. Barbier, Liquid metal embrittlement: a state-of-the-art appraisal. Eur. Phys. J. Appl. Phys. **5**(1), 19–31 (1999)

2. W.F. Savage, E.F. Nippes, R.P. Stanton, Intergranular attack of steel by molten copper. Weld. Res. Suppl. **57**, 9s–16s (1978)